Heliyon 7 (2021) e07024

Contents lists available at ScienceDirect

Heliyon

journal homepage: www.cell.com/heliyon

Research article

Synthesis and evaluation of the *in vitro* and *in vivo* antitrypanosomal activity of 2-styrylquinolines

Roger Espinosa [a], Sara Robledo [b], Camilo Guzmán [a,*], Natalia Arbeláez [b], Lina Yepes [b], Gílmar Santafé [c], Alex Sáez [d]

[a] *IDEFARMA – Department of Regency and Pharmacy, University of Córdoba, Montería, Colombia*
[b] *PECET – Faculty of Medicine, University of Antioquia, Medellin, Colombia*
[c] *Department of Chemistry, University of Córdoba, Montería, Colombia*
[d] *Department of Biological Sciences, EAFIT University, Medellin, Colombia*

ARTICLE INFO

Keywords:
Chagas disease
Trypanosoma cruzi
Antiprotozoal activity
2-styrylquinolines
Antitrypanosomal activity

ABSTRACT

In this study, we report the synthesis and evaluation of *in vitro* and *in vivo* antitrypanosomal activity of styrylquinoline-like compounds (SQ) **3a-h**. Synthesis was carried out by using quinaldine and 8- hydroxyquinaldine with a variety of aromatic aldehydes. The structure of SQs was corroborated by one and two-dimension NMR spectroscopy. *In vitro* antitrypanosomal activity on *T. cruzi* Talahuen strain was evaluated using β-galactosidase enzymatic method; cytotoxicity on U-937 cells was assessed by using MTT [3-(4,5-dimethylthiazol-2-yl)-2,5-diphenyltetrazolium bromide] method. On the other hand, *in vivo* therapeutical response to **3a-f** compounds was evaluated in BALB/c mice (*Mus musculus*) experimentally infected with *T. cruzi* blood trypomastigotes and then orally administered with 100 mg/kg weight day for 20 days. All of the compounds showed *in vitro* activity with EC_{50} values ranging between 4.6 ± 0.1 μg/mL (14.4 μM) and 36.6 ± 6.1 μg/mL (91 μM). Furthermore, treatment with **3a-f** compounds for 20 days resulted in improvement in all of the mice, with a 83–96% decrease in parasitic load at day 90 post-treatment. Treatment with benznidazol (BZ) managed to cure 100% of the mice at the end of treatment. None of the treatments affected the weight of the animals or alanine aminotransferase (ALT), blood urea nitrogen (BUN) and creatinine levels in serum. These results suggest a therapeutic potential of **3a-f** compounds as treatment for the infection.

1. Introduction

Chagas disease (CD) is caused by the hemoflagelated protozoan *Trypanosoma cruzi*, being part of the 17 neglected tropical diseases (NTD) listed by WHO and it is present in 21 Latin American countries, where it represents a public health issue since a high percentage of the population is at risk of infection [1, 2]. Transmission is produced through hematophagous insects belonging to Reduviidae family, but also occurs via blood transfer, organ transplant, shared use of syringes, orally by ingest of contaminated food or beverages and by maternal vertical transmission. nowadays, CD has expanded to non-endemic countries as a consequence of the migration of infected individuals [3, 4, 5, 6].

Treatment for this disease is limited to only two nitroheterocyclic drugs, Benznidazol (BZ) and Nifurtimox (NF) (Figure 1) [7, 8, 9], which only have been efficient in acute or relatively recent chronic infections. Efficacy of both drugs is considered low (0–19%) during chronic phase of the disease. Furthermore, important side effects leading to limitations in patient's treatment finalization have been associated to these drugs [10, 11, 12]. 10000 deaths per year and 8–8.5 million people are estimated to be infected by *T. cruzi* globally. The European Medicines Agency's Scientific Committee for Medicinal Products for Human Use (CHMP) approved the use of Fexinidazol (FX) at the end of 2018 (Figure 1) as the first oral drug for the treatment of Human African Trypanosomiasis (HAT), also known as “sleeping sickness”. Despite the efficacy of FX, relapsing has been observed in some patients, indicating that FX does not generate a parasitological cure in all patients. Besides inducing vomiting and nausea and its absorption depends on food ingest [13, 14, 15, 16, 17]. It is necessary to insist and persevere in the search for new low-cost, safe and effective drugs in order to achieve its mass-scale application and therefore control CD in Colombia and several other countries suffering with this disease.

* Corresponding author.
E-mail address: cantonioguzman@correo.unicordoba.edu.co (C. Guzmán).

https://doi.org/10.1016/j.heliyon.2021.e07024
Received 19 February 2021; Received in revised form 5 April 2021; Accepted 6 May 2021

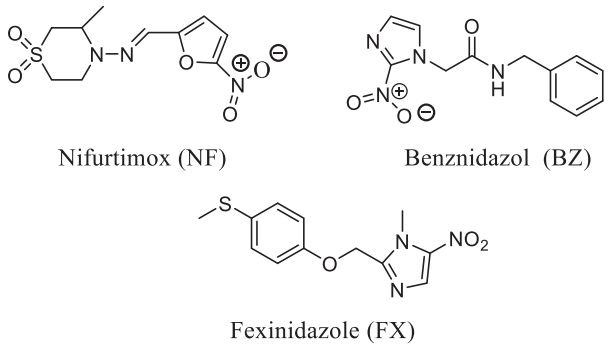

Figure 1. Drugs used in the treatment of infection by *T. cruzi* and The Human African Trypanosomiasis (HAT).

In this context, the compounds with a quinoline nucleus belong to a diverse group of nitrogenated heterocycles prominent for their various pharmacological functions as antiplasmodial, antitumoral, leishmanicidal, among others [18, 19, 20, 21, 22, 23]. Styrylquinolines (SQ) represent an alternative in the obtaining of chemical structures with potential applications in drug development against several infections, including those caused by parasites. Previous studies have demonstrated the potential of several SQ compounds against protozoa parasites such as *Plasmodium falciparum* [24], *Leishmania panamensis* [25, 26] and *Trypanosoma cruzi* [27]. In 2010, Garcia et al. demonstrated that the SQ (*E*)-2-(2,3-dimetoxystyryl) quinoline presented a promising inhibitory activity against *T. cruzi* strain HA trypomastigotes, inhibiting the presence of the parasite in 34.1% compared to the inhibition of 48.7% caused by BZ [28]. In 2015, Coa et al. reported promising activity of hydrazine 2-substituted quinolines against *T. cruzi* intracellular amastigotes by inhibiting parasitaemia in 50.4% using concentrations lower than 10 mg/mL [28]. Finally, given the potential anti-leishmania (*L. panamensis* and *L. braziliensis*) and anti-*Trypanosoma cruzi* [29] activity shown by 2-SQ compounds, the scope of this study was to obtain 2-SQ-like compounds by organic synthesis and to validate the *in vitro* and *in vivo* activity against *T. cruzi* infection. Therefore, these compounds are expected to contribute to the development of newer and more efficient therapeutic alternatives for the treatment of infection by *T. cruzi* on an undetermined phase and therefore prevent the apparition of irreparable damage of cardiac and gastrointestinal organs.

2. Materials and methods

2.1. Chemistry

Chemical structure of SQs was corroborated using specters of Nuclear Magnetic Resonance in one dimension: ^{13}C, ^{1}H, DEPT-135; and for two dimensions: COSY, HSQC, and HMBC. For that matter, a Bruker 300 MHz spectrometer was used with deuterated chloroform ($CDCl_3$) as a solvent and tetramethylsilane [$(CH_3)_4Si$] as an internal standard. Chemical shift (δ) are expressed in parts per million (ppm) and coupling constants (J) in Hertz (Hz). For column chromatography, silica gel 60 was used (0.063–0.200 mm) and silica gel microplates (Merck Kiesegel 60 F_{254}) for thin-layer chromatography. Used grade reagents and solvents were purchased from Merck and Sigma-Aldrich.

2.2. General method of synthesis of styrylquinolines (SQs) 3a-h

A respective aldehyde 2a-g was added to the solution of the corresponding quinaldine **1a,b** in acetic anhydride and the resulting solution was refluxed for 12–24 h. Upon reaction completion (TLC monitor), the reaction mixture was allowed to cool down at room temperature and then a saturated sodium bicarbonate solution was added slowly into the mixture, until complete hydrolysis. Then, the mixture was extracted with petroleum benzine: ethyl acetate, 1:2, and the organic phase was dried under anhydrous sodium sulfate. The solvent was concentrated under reduced pressure and the residue was further purified by a gradient column chromatography, using a mixture of petroleum benzine: ethyl acetate, as eluent [26, 27].

2-[(*E*)-2-(Quinolin-2-yl)ethenyl]phenylacetate (**3a**) was obtained in form of white crystals with a yield of 40%; ^{1}H-NMR ($CDCl_3$): δ 2.43 (s, 3H, CH_3CO), 7.60 (d, 1H, J = 8.5 Hz, Ar–H_3), 8.08 (d, 1H, J = 8.5 Hz, Ar–H_4), 7.79 (d, 1H, J = 8.8 Hz, Ar–H_5), 7.50 (t, 1H, J = 7.5 Hz, Ar–H_6), 7.70 (t, 1H, J = 7.6 Hz, Ar–H_7), 8.13 (d, 1H, J = 8.6 Hz, Ar -H_8), 7.74 (d, 1H, J = 16.4 Hz, $H_{1'}$), 7.42 (d, 1H, J = 16.4 Hz, $H_{2'}$), 7.28 (d, 1H, J = 9.0 Hz, Ar – $H_{3''}$), 7.81 (dt, 1H, J = 8.3; 10.2 Hz, Ar–$H_{4''}$), 7.34 (dt, 1H, J = 6.1; 6.8 Hz, Ar–$H_{5''}$), 7.14 (dd, 1H, J = 7.8; 7.9 Hz, Ar – $H_{6''}$), ^{13}C- NMR ($CDCl_3$): δ 21.20 (CH_3CO), 169.37 (C=O), 155.60 (C-2), 119.2 (C-3), 129.40 (C-4), 129.10 (C-4a), 127.53 (C-5), 126.40 (C-6), 129.80 (C-7), 136.50 (C-8), 148.67 (C-8a), 127.71 (C-1′), 131.23 (C-2'), 127.40 (C-1″), 148.12 (C-2″), 126.3 (C-3″), 127.00 (C-4″), 129.47 (C-5″), 122.9 (C-6").

2-[(*E*)-2-(8-Hydroxyquinolin-2-yl)ethenyl]phenylacetate (**3b**), was obtained as a yellow solid at a 71% yield, ^{1}H NMR ($CDCl_3$, 300MHz): δ 2.42 (s, 3H, CH_3CO), 7.60 (d, 1H, J = 8.5 Hz, Ar–H_3), 8.14 (d, 1H, J = 8.6 Hz, Ar – H_4), 7.79 (d, 1H, J = 7.8 Hz, Ar – H_5), 7.39 (t, 1H, J = 7.5 Hz, Ar – H_6), 7.36–7.25 (m, 1H, Ar – H_7), 7.75 (d, 1H, J = 16.0 Hz, $H_{1'}$), 7.42 (d, 1H, J = 16.0 Hz, $H_{2'}$), 7.36–7.25 (m, 1H, Ar – $H_{3''}$), 7.18 (dd, 1H, J = 7.5; 7.6 Hz, Ar – $H_{4''}$), 7.14 (dd, 1H, J = 8.0; 7.8 Hz, Ar – $H_{5''}$), 7.36–7.25 (m, 1H, Ar – $H_{6''}$). ^{13}C NMR ($CDCl_3$): δ 21.17 (CH_3CO), 169.26 (C=O), 153.24 (C-2), 120.49 (C-3); 136.80 (C-4), 129.03 (C-4a), 127.17 (C-5); 127.80 (C-6), 151.96 (C-8); 148.76 (C-8a), 127.70 (C1′), 127.70 (C2′),129.03 (C-1″); 151.96 (C-2″), 126.30 (C-3″), 110.47 (C4"); 122.9 (C5″).

2-Methoxy-6-[(*E*)-2-(quinolin-2-yl)ethenyl]phenylacetate (**3c**) was obtained as a white solid with a yield of 87%, ^{1}H NMR ($CDCl_3$, 300MHz): δ 2.46 (s, CH_3CO), 3.87 (s, OCH_3), 7.67 (d, 1H, J = 8.6 Hz, Ar–H_3), 8.15 (d, 1H, J = 8.6 Hz, Ar – H_4), 7.80 (d, 1H, J = 8.1 Hz, Ar – H_5), 7.52 (t, 1H, J = 7.4 Hz, Ar – H_6), 7.72 (d, 1H, J = 6.2 Hz, Ar – H_7), 8.10 (d, 1H, J = 8.6 Hz, Ar – H_8), 7.74 (d, 1H, J = 16.5 Hz, $H_{1'}$), 7.43 (d, 1H, J = 16.4 Hz, $H_{2'}$), 6.96 (d, 1H, J = 7.9 Hz, Ar – $H_{4''}$), 7.26 (t, 1H, J = 7.9 Hz, Ar – $H_{5''}$), 7.43 (d, 1H, J = 8.0 Hz, Ar – $H_{6''}$). ^{13}C NMR ($CDCl_3$, 75 MHz): δ(ppm) 20.60 (CH_3CO), 56.02 (OCH_3), 168.45 (C=O), 155.64 (C-2), 119.27 (C-3), 136.33 (C-4), 127.41 (C-4a), 127.54 (C-5), 126.31 (C-6), 129.65 (C-7), 129.29 (C-8), 148.15 (C-8a), 127.36 (C-1′), 131.58 (C-2'), 130.38 (C-1″), 138.17 (C-2″), 151.45 (C-3″), 112.07 (C-4″), 126.48 (C-5″), 118.22 (C-6").

2-Methoxy-6-[(*E*)-2-(8-hydroxyquinolin-2-yl)ethenyl]phenylacetate (**3d**) was obtained as a white solid with a yield of 90%, ^{1}H NMR ($CDCl_3$, 300MHz): δ 2.48 (s, 3H, CH_3CO), 3.90 (s, 3H, OCH_3), 7.64 (d, 1H, J = 8.6 Hz, Ar–H_3), 8.15 (d, 1H, J = 8.6 Hz, Ar – H_4), 7.33 (d, 1H, J = 8.3 Hz, Ar – H_5), 7.23 (dd, 1H, J = 8.3; 7.5 Hz, Ar – H_6), 7.47 (d, 1H, J = 8.0 Hz, Ar – H_7), 7.77 (d, 1H, J = 16.5 Hz, $H_{1'}$), 7.38 (d, 1H, J = 16.5 Hz, $H_{2'}$), 7.45 (d, 1H, J = 8.0 Hz, Ar – $H_{4''}$), 7.28 (t, 1H, J = 8.0 Hz, Ar – $H_{5''}$), 6.99 (d, 1H, J = 8.0 Hz, Ar – $H_{6''}$). ^{13}C NMR ($CDCl_3$): δ 20.32 (CH_3CO), 56.18 (OCH_3),168.87 (C=O), 153.23 (C-2), 120.35 (C-3), 136.52 (C-4), 130.22 (C-4a), 117.54 (C-5), 110.15 (C-6), 127.38 (C-7), 138.18 (C-8), 151.96 (C-8a), 127.38 (C-1′), 130.72 (C-2'), 127.49 (C-1″), 151.47 (C-2″), 151.47 (C-3″), 118.41 (C-4″), 126.68 (C-5″), 111.90 (C-6″).

4-Bromo-2-[(*E*)-2-(quinolin-2-yl)ethenyl]phenylacetate (**3e**) was obtained as white crystals at a yield of 90%, ^{1}H- NMR ($CDCl_3$, 300MHz): δ 2.34 (s, 3H, CH_3CO), 7,63 (d, 1H, J = 8.8 Hz, Ar–H_3), 8.01 (d, 1H, J = 9,4 Hz, Ar – H_4), 7.71 (d, 1H, J = 8.0 Hz, Ar – H_5), 7.45 (t, 1H, J = 7.1 Hz, Ar – H_6), 7.50 (d, 1H, J = 8,5 Hz, Ar – H_7), 8.04 (d, 1H, J = 8.9 Hz, Ar – H_8), 7.60 (d, 1H, J = 16.3 Hz, $H_{1'}$), 7.28 (d, 1H, J = 16.3 Hz, $H_{2'}$), 6,94 (d, 1H, J = 8,6 Hz, Ar – $H_{3''}$), 7.36 (d, 1H, J = 8.6 Hz, Ar – $H_{4''}$), 7,86 (s, 1H, Ar – $H_{6''}$) ^{13}C- NMR ($CDCl_3$): δ 20.94 (CH_3CO), 168.92 (C=O), 154.92 (C-2),

129.35 (C-3), 129.35 (C-4), 129.67 (C-4a), 127.46 (C-5), 126.40 (C-6), 119.53 (C-7), 136.43 (C-8), 148.17 (C-8a), 125.95 (C-1′), 132.17 (C-2’), 119.48 (C-1″), 131.19 (C-2″), 124.54 (C-3″), 131.94 (C-4″), 147.53 (C-5″), 129.68 (C-6”).

2-Ethoxy-4-[(*E*)-2-(quinolin-2-yl)ethenyl]phenylacetate (**3f**) was obtained as white crystals with a yield of 739.4 mg (37%); ^{1}H- NMR ($CDCl_3$, 300MHz): δ 4,14 (q, 2H, J = 6,9 Hz, OCH_2CH_3), 1,42 (t, 3H, J = 6,9 Hz, OCH_2CH_3), 2,32 (s, 3H, CH_3CO), 7.69 (d, 1H, J = 9.0 Hz, Ar–H_3), 8.07 (d, 1H, J = 9.0 Hz, Ar – H_4), 7.77 (d, 1H, J = 8.1 Hz, Ar – H_5), 7.48 (t, 1H, J = 7.5 Hz, Ar – H_6), 7.70 (t, 1H, J = 8.6 Hz, Ar – H_7), 8.11 (d, 1H, J = 9.0 Hz, Ar – H_8), 7.60 (d, 1H, J = 16.0 Hz, $H_{1'}$), 7.36 (d, 1H, J = 16.0 Hz, $H_{2'}$), 7.25 (s, 1H, Ar – $H_{2''}$), 7.17 (d, 1H, J = 8.2 Hz, Ar – $H_{5''}$), 7.05 (d, 1H, J = 8.2 Hz, Ar – $H_{6''}$) ^{13}C- NMR ($CDCl_3$): δ 64.33 (CH_2), 14,71 (CH_3), 20.56 (CH_3CO), 168.93 (C=O), 155.75 (C-2), 119.08 (C-3), 129.10 (C-4), 140.45 (C-4a), 127.51 (C-5), 126.28 (C-6), 129.80 (C-7), 136.48 (C-8), 150.63 (C-8a), 133,84 (C-1′), 129,10 (C-2’), 135,38 (C-1″), 111.34 (C-2″), 148,45 (C-3″), 140.45 (C-4″), 120.48 (C-5″), 122.94 (C-6″).

(*E*)-4-(2-(8-Acetoxyquinolin-2-yl)vinyl)-1,3-phenylene diacetate (**3g**) was obtained as 1210 mg of a white solid with a yield of 61%; ^{1}H- NMR ($CDCl_3$, 300MHz): δ 2.59 (s, 3H, CH_3CO), 2.45 (s, 3H, CH_3CO), 2.34 (s, 3H, CH_3CO), 7.60 (d, 1H, J = 8.6 Hz, Ar - H_3), 8.10 (d, 1H, J = 8.6 Hz, Ar – H_4), 7.60 (dd, 1H, J = 9.2; 1.8 Hz, Ar – H_5), 7.46 (dd, 1H, J = 7.5; 7.7 Hz, Ar – H_6), 7.45 (dd, 1H, J = 7.7; 2.1 Hz, Ar – H_7), 7.28 (d, 1H, J = 16.8 Hz, Ar – $H_{1'}$), 7.70 (d, 1H, J = 16.4 Hz, Ar – $H_{2'}$), 6.90 (d, 1H, J = 2.2 Hz, Ar - $H_{3''}$), 7.06 (dd, 1H, J = 8.6; 2.1 Hz, Ar – $H_{5''}$), 7.76 (d, 1H, J = 8.6 Hz, Ar – $H_{6''}$) ^{13}C NMR ($CDCl_3$): δ (ppm) 21.19 (8-CH_3, CH_3CO), 21.01 (2-CH_3, CH_3CO), 20.07 (3-CH_3, CH_3CO), 169.90 (C=O), 168.95 (C=O, 4-CH_3CO), 168.89 (C=O, 2- CH_3CO), 155.33 (C-2), 120.50 (C-3), 136.60 (C-4), 128.87 (C-4a), 125.40 (C-5), 121.50 (C-6), 125.85 (C-7), 147.32 (C-8), 140.81 (C-8a), 130.70 (C-1′), 127.50 (C-2’), 130.82 (C-1″), 148.85 (C-2″), 116.08 (C-3″), 151.23 (C-4″), 119.50 (C-5″), 127.80 (C-6”).

(*E*)-2-(4-Acetoxy-3-methoxystyryl)quinolin-8-yl acetate (**3h**) was obtained as 250mg of a white solid with a yield of 26%; ^{1}H- NMR ($CDCl_3$, 300MHz): δ 3.95 (s, 3H, OCH_3), 2.61 (s, 3H, CH_3CO), 2,38 (s, 3H, CH_3CO), 7.65 (d, 1H, J = 7.4 Hz, Ar – H_3), 8.15 (d, 1H, J = 8.4 Hz, Ar – H_4), 7.52 (d, 1H, J = 7.5 Hz, Ar – H_5), 7.48 (dd, 1H, J = 7.2; 7.0 Hz, Ar – H_6), 7.69 (d, 1H, J = 6.2 Hz, Ar – H_7), 7.32 (d, 1H, J = 16,2 Hz, $H_{1'}$), 7.66 (d, 1H, J = 18 Hz, $H_{2'}$), 7.25 (s, 1H, Ar – $H_{2''}$), 7.11 (d, 1H, J = 8.1 Hz, Ar – $H_{5''}$), 7.21 (d, 1H, J = 8.3 Hz, Ar – $H_{6''}$) ^{13}C- NMR ($CDCl_3$): δ 21.06 (8-CH_3, CH_3CO), 21.42 (4″- CH_3, CH_3CO), 56.28 (CH_3,-OCH_3), 170.23 (C=O, 8 - CH_3CO), 169.37 (C=O, 4 - CH_3CO), 155.79 (C-2), 119.99 (C-3), 136.59 (C-4), 141.29 (C-4a), 125.85 (C-5), 121.45 (C-6), 125.36 (C-7), 147.54 (C-8), 147.25 (C-8a), 129.27 (C-1′), 134.15 (C-2′), 140,03 (C-1″), 110.23 (C-2″), 151.23 (C-3″), 140.16 (C-4″), 122.42 (C-5″), 120.48 (C-6″).

2.3. Biological activity assays

2.3.1. Preparation of the compounds

The styrylquinolines (SQ) were solubilized in 0.5% dimethyl sulfoxide (DMSO) (Sigma-Aldrich, St Louis MO, USA). Then a 100 μg/mL solution was prepared in RPMI medium (Gibco, Thermo Scientific Inc., Waltham, MA, USA). Four quadruple serial dilutions of each synthesized SQ and BZ (utilized as standard treatment) equivalent to 100, 25, 6.25, y 1.562 μg/mL were prepared.

2.3.2. Parasites

Beta-galactosidase transfected *T. cruzi* Talahuen strain was provided by F. Buckner (University of Washington, WA, USA). Epimastigotes were grown in Novy-MacNeil-Nicolle (NNN) biphasic medium with saline solution buffered with PBS + glucose at pH 6.9 in liquid phase. Cultures were kept on incubation at 26 °C. Cultures to be assayed for β-galactosidase activity were grown in RPMI 1640 medium without phenol red (Gibco BRL) plus 10% FBS, glutamine, penicillin and streptomycin [30]. In order to guarantee a greater *in vitro* macrophage infection, *T. cruzi* strain was reactivated using successive U937 cells infection with epimastogotes and incubation at 37.5% CO_2 until trypomastigotes to be used for infecting U937 macrophages were obtained.

2.3.3. Cells

Human monocytes from U-937 line (ATCC-CRL-1593-2™) were cultured in suspension in RPMI-1640 complete medium, supplemented with 10% fetal bovine serum (FBS) (Invitrogen) and 1% of an antibiotic mixture composed by penicillin (10,000 U/mL) and streptomycin (10,000 U/mL) (Sigma), incubated at 37 °C with 5% CO_2.

2.4. In vitro cytotoxicity of the SQ 3a-h in macrophages of U-937 cells assays

In order to determine the cytotoxicity and toxic effects of SQs and BZ on host cells, human macrophage U937 (American Type Culture Collection, ATCC: CRL1593-2™) line cells were treated with different concentrations of each compounds.

For cytotoxicity assays, non-infected U937 cells were prepared at 10^5 cells/mL. 100 μL of prepared cells were deposited in each well of a cell-culture 96-well plate (Falcon, Fisher Scientific, Thermo Scientific Inc, Waltham, MA, USA). Then, 100 μL of each of the corresponding concentrations for each compound (SQs and BZ) were added: 200-50-12.5–3.125 μg/mL RPMI-1640 and incubated at 37 °C for 72 h. Viable cell rates were assessed by MTT [3-(4,5-dimethyl-2-thiazolyl)-2,5-diphenyl-2H-tetrazoliumbromide; Sigma-Aldrich] [31] colorimetric assay by adding 10 μL/well of a 5 μg/mL MTT solution (Sigma), plates were then incubated for 3 h at 37 °C. After incubation, 100 μL/well of a 50 % isopropanol (Merck) solution and 10 % dodecyl sodium sulfate (SDS) (Merck-Millipore) were added in order to solubilize formed formazan crystals. Plates were incubated for another 30 min and formazan production (which is proportional to viable cell percentage) was measured in a microplate reader (Varioskan Thermo) at a wavelength of 570 nm. Considering cytotoxicity values, feasible doses were calculated for further trypanocidal effect *in vitro* assays [32, 33, 34].

Cytotoxicity was determined according to the percentage of decrease in viable cell quantity obtained for each of the SQ, BZ or doxorubicin concentrations depending on optical densities obtained from each experimental condition in comparison to O.D of cells not exposed to any of the tested compounds. The decreasing in cell viability, denominated as cellular growth inhibition, was calculated utilizing O.D. values for each of the evaluated conditions using the following equation: $\%viability = [(Exposed\ cells\ D.O\ value \div Non - exposed\ cells\ D.O\ values) \times 100]$D.O values from unexposed cells correspond to 100% viability [32, 35].

Based on viability percentages, mortality percentage was also calculated. This corresponds to the reciprocal of viability (100 – %viability). Lastly, median lethal concentration (LC_{50}) was calculated from mortality percentage values using the dose-response relationship analysis method, Probit using SAS Data Analysis (SAS Institute Cary NC, USA) statistic software. Assays were carried out twice with three replicas for each evaluated concentration [32].

Cytotoxicity of each compound was classified according to LC_{50} values by using the following scale: high cytotoxicity if $LC_{50} < 100$ μg/mL; moderate cytotoxicity: $LC_{50} > 100$–200 μg/mL and low cytotoxicity: $LC_{50} > 200$ μg/mL [36, 37, 38, 39, 40].

2.5. Anti – T. cruzi in vitro assays in intracellular amastigotes

For the analysis of the trypanocidal effect, 96-well tissue culture plates (Costar, Cambridge, Mass.) were seeded with PMA induced U937 macrophages at a concentration of 10^3 per well in 100 μL volumes and incubated for 72 h at 37 °C under a 5% CO_2 atmosphere. Beta-galactosidase-expressing epimastigotes were then added at a concentration of 10:1 (parasites:cell) per well in 50 μL volumes of RPMI-1640. After 24 h, drug compounds were added in serial dilutions in 50 μL volumes of RPMI-1640. Each dilution was tested in triplicate. At 72 h of incubations, the assay was developed by adding CPRG (100 μM final

concentration) and Nonidet P-40 (0.1 % final concentration). Plates were incubated for 4–6 h at 37 °C. Well with β-galactosidase activity turned the media from yellow to red, this was quantified by A_{570} (Varioskan Thermo). Tests were performed in triplicate with control groups of infected and non-treated cells by both compounds evaluated in parallel.

The activity of the substances was obtained by the infection index (% viable parasites). Infection inhibition was defined as the decreasing in the quantity of parasites as a result of the evaluated compounds, was calculated using the following equation: $[(Infected\ and\ \exp osed\ cells\ O.D \div Infected\ but\ non - exposed\ cells\ O > D) \times 100]$where the obtained O.D values for infected cells in absence of treatment corresponds to 100% infection percentage. In turn, infection inhibition percentage corresponds to the reciprocal of infection, meaning. This inhibition percentage was then used to determine the dose effect EC_{50} using SAS Data Analysis (SAS Institute Cary NC, USA) statistical program [32, 35, 41, 42].

Just like cytotoxicity, antitrypanosomal activity was classified according to EC_{50} values as following: high activity: $EC_{50} < 25$ μg/mL; Moderate activity: 25 μg/mL $> EC_{50} <$ 50 μg/mL; low activity: $EC_{50} > 50$ μg/mL.

The selectivity index (SI) was obtained by calculating the ratio between LC_{50} value of MTT assay and EC_{50} (concentration of active substance that reduces the number of parasites in 50%) value of the anti-*T. cruzi* activity test.

2.6. In vivo therapeutic response of compounds SQs 3a-h

2.6.1. Ethical aspects

The Ethic Committee for Animal Experimentation (CEEA) of the Universidad de Antioquia approved all procedures (Act # 131 of February 11, 2020).

2.6.2. Infection of mice

Domestic mouse (*Mus musculus*) endogamic Balb/c strain, specific pathogen-free, 6-week old male and female, maintained with the following macro environment conditions: 22 °C temperature, 60% relative humidity, 16–20 air changes/hour regulated by the facility ventilation system, and white light artificial lighting with 12/12 light/dark cycles regulated by a timer. Micro environmental conditions were as following: for groups of same-sex animals in transparent polypropylene or acrylic containers, 19 cm height x 20 cm width and 30 cm length; filled at two thirds with sterilized wood shavings. Kept with experimentation rodent food and water (LabDiet®) previously sterilized, at will. Forty-two mice were inoculated via intraperitoneal route (IP) with an inoculum of 100 blood tripomastigotes obtained from donor Balb/c mice at the day of parasitaemia peak, counted by hematocrit [41].

2.6.3. Administration schemes

The infection was confirmed by counting the parasitaemia by hematocrit and according to the appearance of the mice who developed piloerection, dehydration and xyphosis posture (Figure 2). Treatments were administered in mice by oral route with the SQ solutions at a 100 mg/kg/day dose. Treatment started in the first day of parasitaemia, which is 30 days after the inoculation of Talahuen strain in infected animals. Mice were randomly distributed in seven groups (n = 6). SQs were prepared in 5% Tween-80 and 5% mineral oil in water. Volumes of 0.2mL of each solution were administered to the treated animals via oral route at a 100 mg/kg/day dose during 25 days. Control groups treated for 25 days with BZ at 100 mg/kg/day and INT groups were included and evaluated in parallel. Clinical follow-up was done daily at the time of dose administration. Body-weight was registered weekly for the duration of the treatment in order to monitor weight-loss and adjust the volume of administered compounds according to weight changes, and then it was monitored at 30, 60 and 90 days post-treatment.

2.6.4. Evaluation of treated animals

The response to treatment was determined according to the parasitaemia (PAR) curve performed at TD0, TD25 (last day of treatment) and PTD30, 60 and 90 using the hematocrit method. The PAR curve was plotted using the parasite number count/0.1mL of blood. Animals that were negative in all parasitological tests were considered cured. The ARRIVE (Animal Research: Reporting of *in vivo* Experiments) guidelines were followed to reporting of research using animals (https://www.nc3rs.org.uk).

2.7. Statistical analyses

Data statistical analyses were performed using Prism software v8 (GraphPad Software, San Diego, CA). Data were initially assessed by one-way analysis of variance (ANOVA). When interactions were significant, a Tukey test was used to determine specific differences between mean values. The Kolgomorov-Smirnov test was used to compare parasitaemia between treated and non-treated infection groups. One-way ANOVA or Mann-Whitney U tests were performed to compare maximum peak values of parasitaemia among the different groups. The log-rank (Mantel-Cox) method was used to estimate the average survival for the different experimental groups. Values were expressed as means of standard deviations. Differences in mean values were considered significant if $P < 0.05$.

3. Results and discussion

3.1. Chemistry

Quinolines **1a** and **1b** were subjected to a condensation reaction with various aromatic aldehydes (**2a-g**) utilizing high temperatures as condition of the reaction and acetic anhydride (Ac_2O), obtaining **3a-h** compounds (Figure 3) with yields ranging between 20 – 90%. Compounds **3b-e** had a high yield with values above 70%, only compounds **3a, 3f, 3g** and **3h** were below this value. This yield decreasing may be attributed to the formation of subproducts, reaction conditions such as

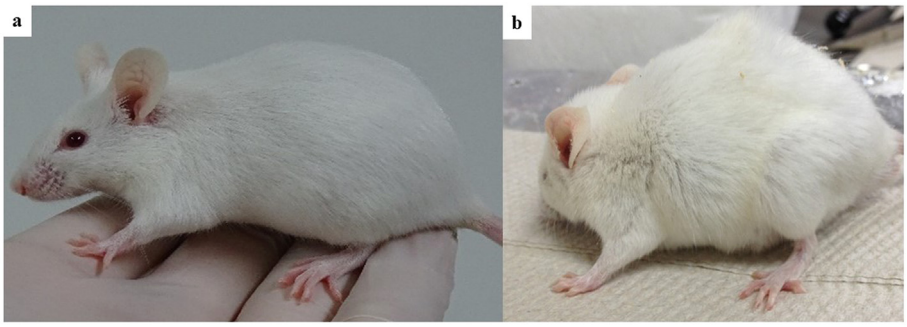

Figure 2. Appearance of healthy Balb/c mice (a) and infected with *T. cruzi*, Tulahuen B-gal strain (b). Note in (b) piloerection, dehydration and xiphosis posture.

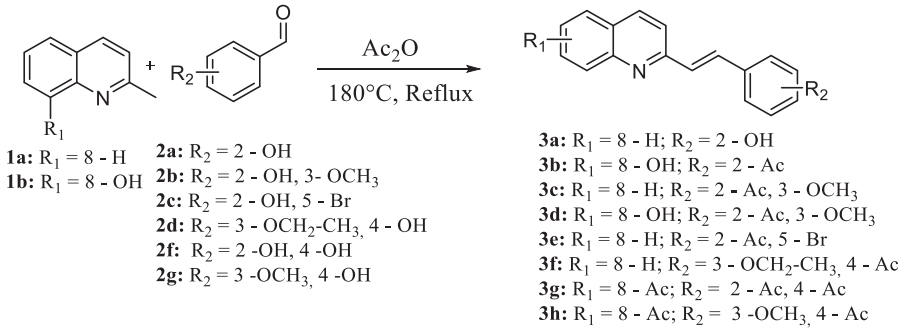

Figure 3. Synthesis route of Styrylquinolines (SQ) **3a-h**.

temperature and duration, as well as the constitution and size of aromatic aldehydes substituents. Synthesis strategy was based in the modification of the aromatic aldehyde (**2a-g**) and the quinoline ring (**1a,b**) [28]. Chemical structure of the compounds were confirmed by one dimension ^{1}H- NMR, ^{13}C -NMR, DEPT 135 and two dimension COSY, HSQC and HMBC spectroscopic methods. (See Supplementary Material Spectra NMR SQ 3 (a-h)).

3.2. Cytotoxicity and antitrypanosomal activity

All of the compounds **3a-h** showed LC_{50} values ranging between 5.9 μg/mL (15.6 μM) and 25.3 μg/mL (40.8 μM), where compounds **3a**, **3g** and **3h** showed higher cytotoxicity (Table 1). In relation to its antitrypanosomal activity, **3a** to **3d** showed high activity against *T. cruzi* with EC_{50} values ranging between 4.6 μg/mL (14.4 μM) and 12.5 μg/mL (40.8 μM) with **3a** and **3c** being the most active compounds. **3e**, **3f**, **3g**, and **3h** showed moderate activity, with EC_{50} values of 34.6 μg/mL (94.0 μM), 27.8 μg/mL (83.0 μM), 36.6 μg/mL (91.0 μM) and 24.2 μg/mL (64.2 μM) respectively (Table 1).

Comparing the structure of the compounds **3a-h** and cytotoxicity, it was observed that the presence of hydroxyl groups (-OH) in position 8 of the quinolone ring resulted in a diminution in the cytotoxicity of the compounds **3b** and **3d**. On the other hand, the presence of oxygenated and electron-giving (acetoxy) substituents in the molecules led to a increase in cytotoxicity (compounds **3a**, **3c**, **3g** and **3h**). The addition of a bromine atom in compound **3e** and a two-carbon atom substituent (etoxy) in compound **3f** produced cytotoxicity decrease; this allows inferring that the addition of substituents with aliphatic chains consisting of more than two carbon atoms, and the deacetylation of acetoxy substituents (Ac) may reduce cytotoxicity in these molecules.

When linking toxicity and antitrypanosomal activity, even though the cytotoxicity of **3a** and **3c** was 22.5 and 21.7 times higher than the cytotoxicity of BZ, the activity showed by these compounds was 2.5 and 3.2 times higher than BZ. Likewise, while **3b** and **3d** toxicity was 12 and 12.3 times higher than BZ, therapeutic activity of these compounds was also 1.17 and 1.22 times higher than BZ respectively. Although all of the compounds showing to be cytotoxic, their antiparasitic activity was much higher as reflected by a selectivity index (SI) with values close to 1 for compounds **3e** – **3f** and greater than one for compounds **3a** – **3d**, this suggests that these compounds probably have more selectivity towards the parasite (Table 1).

Despite cytotoxicity is an important criterion when identifying compounds with terapeutic potential, specific activity is an even more important criterion; in this case antitrypanosomal activity, since cytotoxicity is a property that can be controlled and reduced by using drug-delivery systems such as liposomes among other pharmacological activity enhancer nanoparticles; which allows to overcome issues like limited solubility, drug aggregation, low biodisponibility, low biodistribution, lack of selectivity or lowering drug's side-effects without causing a loss of therapeutic efficacy [41, 43, 44].

When comparing the structure of the compounds **3a-h** and antitripanosomal *in vitro* activity, it was observed that in compounds **3a** - **3d** the absence of hydroxyl groups (-OH) in position 8 of the quinolone ring caused a significative augment in biological activity. In the same sense, the presence of an acetoxy (Ac) group in position 2 of the aromatic ring which results synthetically from aldehyde is directly related to the observed good activity. on the other hand, the addition of an halogen (bromine) in compound **3f**, an etoxyle substituent (-OCH_2CH_3) in compound **3e** in the aromatic ring of the aldehyde, and a acetoxy group (Ac) in position 8 of the quinolone ring lead to a decrease in antitripanosomal in vitro activity. Finally, the presence of a single acetoxy substituent (Ac); in other words, electron givers in the molecule (compound **3g**) provoked a decrease in biological activity.

From the general perspective of the chemical structure of the evaluated molecules, it confirms that styryl and oxygenated (acetoxy) group substitution of position 2 of the quinoline ring notoriously enhances

Table 1. *In vitro* cytotoxicity and anti - *T. cruzi* activity of styrylquinolines (SQ) **3a-h**.

Compounds	LC_{50}^{a}		EC_{50}^{b}		SI[c]
	μg/ml	μM	μg/ml	μM	
3a	8.9 ± 1.8	30.8	5.77 ± 0.1	19.9	1.6
3b	16.7 ± 3.8	54.6	12.5 ± 2.0	40.8	1.3
3c	9.2 ± 1.9	28.8	4.6 ± 0.10	14.4	2.0
3d	16.3 ± 3.5	48.5	12.0 ± 1.0	36.0	1.4
3e	25.3 ± 2.7	68.8	34.6 ± 2.4	94.0	0.7
3f	18.4 ± 0.8	55.2	27.8 ± 3.1	83.5	0.7
3g	6.9 ± 0.2	17.2	36.6 ± 6.1	91.0	0,2
3h	5.9 ± 0.03	15.6	24.2 ± 3.4	64.2	0.2
Benznidazol (BZ)	>200.0 ± N. A	491.0	14.7 ± 0.1	56.5	8.7

The results are reported as mean values ± standard deviation. [a]LC_{50}: Median lethal concentration; [b]EC_{50}: Median effective concentration; [c]SI: Selectivity index = LC_{50}/EC_{50}; N.A: Not Apply.

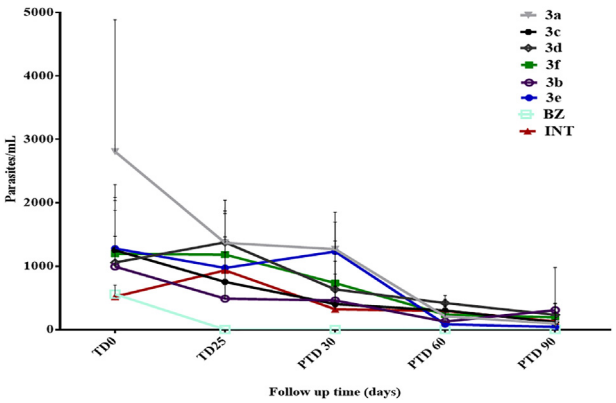

Figure 4. Evolution of mean parasitaemia (#parasites/mL) during the research. Data shows mean values of parasitaemia determined by micro hematocrit concentration method of the six treatment groups, as well as the BZ-treated and non-treated control groups at the beginning and the end of the treatment, then at 30, 60 an0d 90 days post-treatment (PTD30, PTD60 and PTD90 respectively). Mice from BZ-treated control group showed absence of parasites at the end of the treatment, and continued to be negative in post-treatment follow-up, showing evidences of being cured.

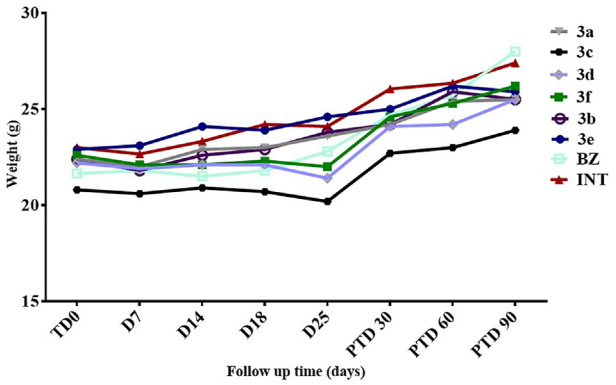

Figure 5. Mean body weight in grams per assay group at the beginning of the treatment, week 1, week 2, week 3, end of treatment and followed-up at post-treatment days 30, 60 and 90 (PTD30, PTD60, PTD90).

antitrypanosomal activity [41]. Even though the physiological mechanism of the activity of SQ on *T. cruzi* has not been described, it has been observed that quinolines with activity should have: an unsaturated structure, for the occurrence of chemical reactions with molecular targets; an alkyl-chain length not exceeding 5 carbons and the presence of functional groups in the substituents with no shared electrons [27, 45, 46].

3.3. *In vivo* therapeutic response of topic formulation of ***3a-f*** compounds

Therapeutic potential of these compounds was validated in Balc/c mice experimentally infected with *T. cruzi*, parasitaemia evolution (PAR) during and after the treatment are observed in Figure 4.

Reduction in parasitaemia was calculated for each mouse in each group, in relation to the parasitaemia before starting the treatment. Then, taking into consideration that mice were in an early undetermined phase at the end of the treatment (day 32 post experimental infection) and the important declining in mice parasitaemia even in absence of treatment, the obtained reduction percentage was normalized for each group by subtracting the percentage showed by INT (infected not treated) group at each stage of the follow-up. After 25 days of a 100 mg/kg/day dose treatment, all of the compounds (except for the **3d**) reduced PAR in 5.7–50.1% (Table 2). On the contrary, compound **3d** increased PAR by 22.7%. In the BZ treated group, parasitaemia was negative at the end of therapy.

Mice were kept in follow-up for 3 months after the end of treatment. At day 30 post-treatment (PTD30), an increase in PAR for all the treated groups was observed; giving negative parasitaemia reduction percentages, with values ranging between -2.7 and -58.9. For the group treated with **3c**, PAR was reduced by 8.4% only (Table 2). At day 60 post-treatment (PTD60), PAR showed a treatment-dependent variable reduction with values between 14.8 and 30.5%. Groups treated with **3c** continued to show a mild increase (-2.5%) in PAR lastly, at day 90 post-treatment (PTD90) PAR showed a greater reduction in all the treatment groups, including **3c** with values ranging between 9.3 and 32.7% (Table 2); with **3e** and **3a** being the most effective compounds with a parasitaemia reduction of 32.7 and 32.5% compared to the no-treatment group, followed by **3c**, **3d**, **3f** with a disminution of 26.0, 24.9 and 21.7% respectively, **3b** was the least effective compound, showing a reduction of only 9.3% at the end of study.

Despite the increase in PAR happening after the ending of treatment, this could be due to the early interruption of the treatment and the following reproduction of the remaining parasites in circulation because of the absence of compound-driven pressure. However, results obtained at PTD60 and PTD90 suggest a therapeutic effect of the compounds that managed to control the multiplication of parasites, leading to a reduction in parasitaemia even in compound **3d** whose PAR was increased at the end of the treatment.

In previous studies, where we demonstrate that for *T. cruzi* (Talahuen strain) infected Balb/c mice model used in this study, acute phase is characterized by a high parasitaemia occurring between day 8 and day 24 post-inoculation, followed by the undetermined phase lasting until D120 post-inoculation and characterized by a 50–60% diminution in parasitaemia compared to acute phase since parasites start lodging in tissue where transformed into amastigotes (data not shown). In this study, mice treatment started at D20 post-inoculation which corresponds to late acute phase and continued for 25 days at undetermined stage of the infection. With that in mind, the effectivity of a compound should not be measured by PAR reduction at the end of the treatment only but by parasitaemia observed during follow-up too. In the last case, comparison must be carried out according to parasitaemia showed by infected and not treated mice, which make up for a 100% of the expected parasitaemia.

Table 2. Effect of SQ compounds **3a-f** in the reduction of parasitaemia per assayed group during the study (%parasitaemia reduction).

Treatment	Follow-up			
	TD25 (%)	PDT30 (%)	PTD60 (%)	PTD90 (%)
3a	49.4	-7.9	29.6	32.5
3b	50.1	-2.7	26.1	9.3
3c	36.5	8.4	14.8	26.0
3d	-22.7	-22.6	-2.5	24.9
3e	16.4	-58.9	30.5	32.7
3f	5.7	-16.6	19.7	21.7
Benznidazol (BZ)	100	100	100	100

3.4. Effect of treatment with SQ on the body weight of mice infected with *T. cruzi*

Mice treated with SQ and BZ did not show alterations or clinical signs of importance after the treatments were administered, this allowed completing the therapeutic scheme for all groups. Dehydration and mild piloerection in response to infection and a non-significant mild weight-loss that did not affect their corporal condition or animal status were found (Figure 5).

At the end of the treatment, groups administered with **3c**, **3d**, and **3f** showed mild weight-loss, this could be due to the stress caused by manipulation during the 25 days of treatment; afterwards these groups managed to recover from weight-loss same as the other groups and showed weight-gains during treatment and post-treatment follow-up. BZ treated group kept a stable mean weight followed by weight-gain in all individuals.

At the end of PTD90 test, CO_2 chamber euthanasia was applied in all the treated groups and necropsy was done in all the individuals. There was no toxicity suggesting macroscopic alterations in any organs also there were no infection-caused injuries.

There was a correlation between the *in vitro* and *in vivo* anti-trypanosomal activity, demonstrating a promissory activity of SQ compounds **3a-f** evidenced in PAR percentage reduction at PTD90. The 25-day administering of SQ compound did not generate visible signs of toxicity in treated mice, also there was no significant weight-loss. Mice maintained an adequate general status. The absence of significant weight-loss, as well as the lack of organ and tissue alteration in none of the treatment groups, suggests that the moderate toxicity of the compounds during the *in vitro* assays was attenuated with intraperitoneal administration.

4. Conclusion

The results obtained in this research suggest that the compounds, specially **3e**, **3a** and **3c** are promissory and could be considered as main compounds in the development of a drug for the oral treatment of infection by *T. cruzi* during undetermined phase. Additional research in the optimization of concentration, formulation and treatment schemes are necessary whether it be applying higher doses or extending the treatment's duration in order to allow complete elimination of the circulating parasites and therefore accomplish an after-treatment 100% reduction in parasitaemia.

Declarations

Author contribution statement

Roger Espinosa, Sara Robledo, Camilo Guzmán, Natalia Arbeláez, Lina Yepes, Gílmar Santafé, Alex Sáez: Conceived and designed the experiments; Performed the experiments; Analyzed and interpreted the data; Contributed reagents, materials, analysis tools or data; Wrote the paper.

Funding statement

This work was supported by University of Córdoba and University of Antioquia (Colombia).

Data availability statement

Data will be made available on request.

Declaration of interests statement

The authors declare no conflict of interest.

Additional information

Supplementary content related to this article has been published online at https://doi.org/10.1016/j.heliyon.2021.e07024.

References

[1] A.E. Bivona, A.S. Alberti, N. Cerny, S.N. Trinitario, E.L. Malchiodi, Chagas disease vaccine design: the search for an efficient *Trypanosoma cruzi* immune-mediated control, Biochim. Biophys. Acta (BBA) - Mol. Basis Dis. 1866 (2020) 165658.
[2] C.B. Scarim, D.H. Jornada, R.C. Chelucci, L. de Almeida, J.L. dos Santos, M.C. Chung, Current advances in drug discovery for Chagas disease, Eur. J. Med. Chem. 155 (2018) 824–838.
[3] M.D. Klein, A. Proaño, S. Noazin, M. Sciaudone, R.H. Gilman, N.M. Bowman, Risk factors for vertical transmission of Chagas disease: a systematic review and meta-analysis, Int. J. Infect. Dis. 105 (2021) 357–373.
[4] G.A. Schmunis, Z.E. Yadon, Chagas disease: a Latin American health problem becoming a world health problem, Acta Trop. 115 (2010) 14–21.
[5] J.R. Coura, Chagas disease: control, elimination and eradication. Is it possible? Mem. Inst. Oswaldo Cruz 108 (2013) 962–967.
[6] S.S. Santos, R.V. de Araújo, J. Giarolla, O.E. Seoud, E.I. Ferreira, Searching for drugs for chagas disease, leishmaniasis and schistosomiasis: a review, Agentes Antimicrobianos Int. J. 55 (2020) 105906.
[7] J.M. Kratz, Drug discovery for chagas disease: a viewpoint, Acta Trop. 198 (2019) 105107.
[8] J.R. Coura, J. Borges-Pereira, Chagas disease. What is known and what should be improved: a systemic review, Rev. Soc. Bras. Med. Trop. 45 (2012) 286–296.
[9] A.K. Soares, P.A. Neves, A.V. Nascimento, A.A. Esmeraldo, L.R. Moreira, T.M. Higino, R.C.B.Q. Figueiredo, M.M. Cavalcanti, S.M. Martins, C. Carrazone, W.O. Júnior, Y.M. Gomes, V.M. Lorena, Benznidazole: Hero or villain of cellular immune response in chronic Chagas disease patients? Immunobiology 226 (2021) 152046.
[10] D.L. Nossa, Gomez J.A. Castano, W.E. Rozo, P.R. Duchowicz, Antiprotozoal QSAR modelling for trypanosomiasis (Chagas disease) based on thiosemicarbazone and thiazole derivatives, J. Mol. Graph. Model. 103 (2021) 107821.
[11] C. Bern, Chagas' disease, Dis. N. Engl. J. Med. 373 (2015) 456–466.
[12] J. Bermúdez, C. Davies, A. Simonazzi, J.P. Real, S. Palma, Current drug therapy and pharmaceutical challenges for Chagas disease, Acta Trop. 156 (2016) 1–16.
[13] K. Lindner, V. Lejon, F. Chappuis, J. Seixas, L. Kazumba, M.P. Barrett, E. Mwamba, O. Erphas, E.A. Akl, G. Villanueva, H. Bergman, P. Simarro, A.K. Ebeja, G. Priotto, J.R. Franco, New WHO guidelines for treatment of gambiense human african trypanosomiasis including fexinidazole: substantial changes for clinical practice, Lancet Infect. Dis. 20 (2019) 1–9.
[14] H. Zhang, J. Collins, R. Nyamwihura, O. Crown, O. Ajayi, I.V. Ogungbe, Vinyl sulfone-based inhibitors of trypanosomal cysteine protease rhodesain with improved antitrypanosomal activities, Bioorg. Med. Chem. Lett. 30 (2020) 127217.
[15] C. Fersing, C. Boudot, C. Castera-Ducros, E. Pinault, S. Hutter, R. Paoli-Lombardo, P. Vanelle, 8-alkynyl-3-nitroimidazopyridines display potent antitrypanosomal activity against both *T. b. brucei* and *cruzi*, Eur. J. Med. Chem. 202 (2020) 112558.
[16] C. Poveda, M.E. Bottazzi, K.M. Jones, Mining the metabolome for new and innovative chagas disease treatments, Trends Pharmacol. Sci. 42 (2021) 1–3.
[17] M. Bahia, L. De Figueiredo, V. Furtado, Therapeutical approaches under investigation for treatment of Chagas disease, Expet Opin. Invest. Drugs 9 (2014) 2–13.
[18] A. Mrozek-Wilczkiewicz, M. Kuczak, K. Malarz, W. Cieślik, E. Spaczyńska, R. Musiol, The synthesis and anticancer activity of 2-styrylquinoline derivatives. A p53 independent mechanism of action, Eur. J. Med. Chem. 177 (2019) 338–349.
[19] X. Chu, C. Wang, W. Liu, L. Liang, K. Gong, C. Zhao, K. Sun, Quinoline and quinolone dimers and their biological activities: an overview, Eur. J. Med. Chem. 161 (2019) 101–117.
[20] A. Marella, O. Tanwar, R. Saha, M. Ali, S. Srivastava, M. Akhter, M. Shaquiquzzaman, M. Alam, Quinoline: a versatile heterocyclic, Saudi Pharmaceut. J. 21 (2013) 1–12.
[21] B. S Matada, R. Pattanashettar, N. Yernale, Comprehensive review on the biological interest of quinoline and its derivatives, Bioorg. Med. Chem. 32 (2021) 115973.
[22] N. Pavlidis, A. Kofinas, M.G. Papanikolaou, H.N. Miras, C. Drouza, A.G. Kalampounias, G. Leondaritis, Synthesis, characterization and pharmacological evaluation of quinoline derivatives and their complexes with copper (II) in *in vitro* cell models of Alzheimer's disease, J. Inorg. Biochem. (2021) 111393.
[23] M. Wang, G. Zhang, J. Zhao, N. Cheng, Y. Wang, Y. Fu, Y. Wang, Synthesis and antiviral activity of a series of novel quinoline derivatives as anti-RSV or anti-IAV agents, Eur. J. Med. Chem. 214 (2021) 113208.
[24] G. Santafé, E. Sánchez, O. Torres, Synthesis and antimalarial activity of styrylquinolines on *Plasmodium falciparum*, Inf. Tecnol. 27 (2016) 97–104.
[25] E.L. Sánchez, G.G. Santafé, O.L. Torres, D.L. Muñoz, S.M. Robledo, Synthetic compounds type styrylquinoline with leishmanicidal and cytotoxic activities, Biomedica 3 (2014) 605.
[26] P. Cantero, S.M. Robledo, O. Yañez, C. Zúñiga, G.G. Santafé, Theoretical study of new LmDHODH and LmTXNPx complexes: structure-based relationshipsl, Struct. Chem. 32 (2021) 167–177.
[27] P. García, C. Genes, P. Molano, O. Torres, J. Saez, O. Triana, Evaluation of the trypanocidal, cytotoxic and genotoxic activity of styrylquinoline analogs, J. Chemother. 22 (2010) 169–174.
[28] J. Coa, W. Castrillon, W. Cardona, M. Carda, V. Ospina, J. Muñoz, I. Vélez, S. Robledo, Synthesis, leishmanicidal, trypanocidal and cytotoxic activity of quinoline-hydrazone hybrids, Eur. J. Med. Chem. 101 (2015) 746–753.

[29] R. Espinosa, O. Torres, S. Robledo, Patente de Invención, Superintendencia de Industria y Comercio, Colombia, 2020. Resolución No. 13586.
[30] F.S. Buckner, C.L. Verlinde, A.C. La Flamme, W.C. Van Voorhi, Efficient technique for screening drugs for activity against *Trypanosoma cruzi* using parasites expressing beta-galactosidase, Antimicrob. Agents Chemother. 40 (1996) 2592–2597.
[31] F.M. Freimoser, C.A. Jakob, M. Aebi, U. Tuor, The MTT [3-(4,5-dimethylthiazol-2-yl)-2,5-diphenyltetrazolium bromide] assay is a fast and reliable method for colorimetric determination of fungal cell densities, Appl. Environ. Microbiol. 65 (1999) 3727–3729.
[32] J.D. Finney, Statistical logic in the monitoring of reactions to therapeutic drugs, Methods Inf. Med. 10 (1971) 237–245.
[33] W. Cardona, S. Robledo, F. Álzate, C. Yepes, I. D Vélez, J.C. Calderón, I. Vásquez, Antileishmanial and cytotoxic activities of four Andean plant extracts from Colombia, Vet. World 13 (2020) 2178–2182.
[34] J.A. Murillo, J.F. Gil, Y.A. Upegui, A.M. Restrepo, S.M. Robledo, W. Quiñones, G. Escobar, Antileishmanial activity and cytotoxicity of ent-beyerene diterpenoids, Bioorg. Med. Chem. 1 (2019) 153–160.
[35] B. Insuasty, And twelve other authors, an efficient synthesis of new caffeine-based chalcones, pyrazolines and pyrazolo[3,4-b][1,4]diazepines as potential antimalarial, antitrypanosomal and antileishmanial agents, Eur. J. Med. Chem. 93 (2015) 401–413.
[36] A. Rios-Vasquez, R.O. Cardona, S.M. Duque, S. Restrepo, I. Bernal, D. Medina, M.A. Jones, U.S. Patent No. 9,145,352, U.S. Patent and Trademark Office.e, Washington, DC, 2015.
[37] S.M. Duque, L.A. Ríos, R. Ocampo, D.L. Cedeno, M.A. Jones, I.D. Velez, S.M. Robledo, Synthesis of novel quaternary ammonium salts and their in vitro antileishmanial activity and U-937 cell cytotoxicity, Molecules 21 (4) (2016) 381.
[38] M. Fernández, J. Murillo, L.A. Ríos-Váasquez, R. Ocampo-Cardona, D.L. Cedeño, M.A. Jones, I.D. Vélez, S.M. Robledo, *In Vivo* studies of the effectiveness of novel N-halomethylated and non-halomethylated quaternary ammonium salts in the topical treatment of cutaneous leishmaniasis, Parasitol. Res. 117 (1) (2018) 273–286.
[39] S.A. Pulido, V.H. Nguyen, J.F. Alzate, D.L. Cedeno, M.A. Makurath, A. Ríos, J.A. Friesen, Insights into the phosphatidylcholine and phosphatidylethanolamine biosynthetic pathways in *Leishmania* parasites and characterization of a choline kinase from *Leishmania infantum*, Comp. Biochem. Physiol. B Biochem. Mol. Biol. 213 (2017) 45–54.
[40] C.V. Mesa, G.A. Blandon, D.L. Munoz, C.E. Muskus, A.F. Florez, R. Ochoa, S.M. Robledo, *In silico* screening of potential drug with antileishmanial activity and validation of their activity by *in vitro* and *in vivo* studies, J. Chem. Eng. 9 (2015) 375–402.
[41] Y. Upegui, S.M. Robledo, J. Gil, W. Quiñones, R. Archbold, F. Torres, G. Escobar, B. Nariño, F. Echeverri, In v*ivo ant*imalarial activity of α-Mangostin and the new Xanthone δ-Mangostin, Phytother Res. 29 (2015) 1195–1201.
[42] E. Otero, E. García, G. Palacios, L. Yepes, M. Carda, R. Agut, S.M. Robledo, Triclosan-caffeic acid hybrids: synthesis, leishmanicidal, trypanocidal and cytotoxic activities, Eur. J. Med. Chem. 141 (2017) 73–83.
[43] L. Chong, W. Jiancheng, W. Yiguang, G. Huile, W. Gang, H. Yongzhuo, Y. Haijun, G. Yong, W. Yongjun M. Lin, C. Huabing, H. Haiyan, Z. Zhiping, J. Yiguang, Recent progress in drug delivery, Acta Pharm. Sin. B 9 (2019) 1145–1162.
[44] J.P. Botero, A.M. Restrepo, Amphotericin B deoxycholate versus liposomal amphotericin B: effects on kidney function, Cochrane Database Syst. Rev. 23 (2015).
[45] M. Fakhfakh, A. Fournet, E. Prina, M. Francois, X. Franck, R. Hocquemiller, Synthesis and biological evaluation of substituted quinolines: potential treatment of protozoal and retroviral co-infections, Bioorg. Med. Chem. 11 (2003) 5013–5023.
[46] H. Nakayama, P.M. Loiseau, C. Bories, S. Torres, A. Schinini, E.W. Serna, A. Fournet, Efficacy of orally administered 2-substituted quinolines in experimental murine cutaneous and visceral leishmaniases, Antimicrob. Agents Chemother. 49 (2005) 4950–4956.